

Supplementary Information Appendix for

**TUMOR REGRESSION AND RESISTANCE MECHANISMS UPON CDK4 AND
RAF1 INACTIVATION IN KRAS/P53 MUTANT LUNG ADENOCARCINOMAS**

Laura Esteban-Burgos, Haiyun Wang, Patricia Nieto, Jie Zheng, Carmen Blanco-Aparicio, Carmen Varela, Gonzalo Gómez-López, Fernando Fernández-García, Manuel Sanclemente, Carmen Guerra, Matthias Drosten, Javier Galán, Eduardo Caleiras, Jorge Martínez-Torrecuadrada, Lluís Fajas, Sheng-Bin Peng, David Santamaría, Monica Musteanu and Mariano Barbacid

Correspondence: mmusteanu@cniio.es and mbarbacid@cniio.es

This PDF file includes:

SI Appendix Materials and Methods

SI Appendix Figures S1 to S8

SI Appendix Figure Legends S1 to S8

SI Appendix Tables S1 to S3

SI Appendix Materials and Methods

Tumor genotyping. Semiquantitative genotyping was performed using nested PCR. The first PCR contains each locus-specific primer needed to detect the ratio between unrecombined (FxD/L) versus recombined (KD/-) alleles. For the second real time PCR (RT-PCR), the first PCR products were diluted 1:20 in water and used as a 5x stock. The RT-PCR was prepared with fluorescent reporter-quencher custom probes indicated by an asterisk (see below). All reactions were performed in triplicate. Results were analyzed with the CFX Maestro Software (BioRad). Firstly, thresholds are separately set for each fluorophore channel lying above their respective general noise but still within the curves' linear range and subsequently taken to the same consensus value within their ranges. The cycle number where its amplification curves cross the common threshold (Cq as determined in "single threshold" mode) is taken, and used to estimate allele frequencies. Cq values for *Cdk4*^{FxD/L} and *Cdk4*^{KD/-} alleles are averaged among sample replicates, and these two averages are subtracted from one another. The absolute value of this resulting delta Cq is used to estimate the corresponding fold differences between the unrecombined and recombined alleles abundance in the sample. Oligonucleotides (Integrated DNA Technologies Inc.) used for sample genotyping were:

<i>Cdk4</i> ^{KD}		
GGTGGAGAGGACAATAGGAC	KD	Fw primer
AAACGCTAGTGAGCTCGA	FxD	Fw primer
GAACAAATGATCACCAGCTAGTC	FxD, KD	Rev primer
TTGAACATCCCAATGTTGTACG	KD	Fw primer(*)
GGAACCTCTGCACAAGGT	FxD	Fw primer(*)
CAGACATCCATCAGCCTGA	FxD, KD	Rev primer(*)
Fam-CGGATCCATCGACCCATAACTT-IowaBlack	FxD	probe
Cy5/Fam-CGTTGAGGATCTTCTAGAGCTTATAA-IowaBlack	KD	probe

<i>Cdk4^L</i>		
GCCATCTCTCCAGTCCTGTA	L	Fw primer
GCAGTCTCATCCAGGATCG	–	Fw primer
ACTCTGTCAGCGCTGTATTAC	–	Rev primer
GTTATATTATGTACCGAAGTTCCTATACT	L	Rev primer
TGCTCTTAGCTGCTGAGC	L	Fw primer(*)
GAGCGTAAGGTGAGTGCA	–	Fw primer(*)
GCCTTCCATCTCATTGGAGAC	L, –	Rv primer(*)
Fam-ATCGAATTCCGAAGTTCCTATTCTC-IowaBlack	L	probe
Cy5/Fam-CCGCATTCTGGTACCAGGGC-IowaBlack	–	probe
<i>Raf1^L</i>		
AGACATCCAGAGACAGGCA	L	Fw primer
CTTGGATCCACTAGTTCTAGAGC	–	Fw primer
CAGCAGTTAGGTAAGCAGGC	L, –	Rev primer
CTGATTGCCCAACTGCCATAA	L	Fw primer(*)
CACGATGCATGTAACCTGTGT	–	Fw primer(*)
ACTGATCTGGAGCACAGCAAT	L, –	Rev primer(*)
Fam-AGCTCTGCAGATAACTTCGT-IowaBlack	L	probe
Cy5/Fam-TAGACTCGAGGAATTCCGATCATA-IowaBlack	–	probe

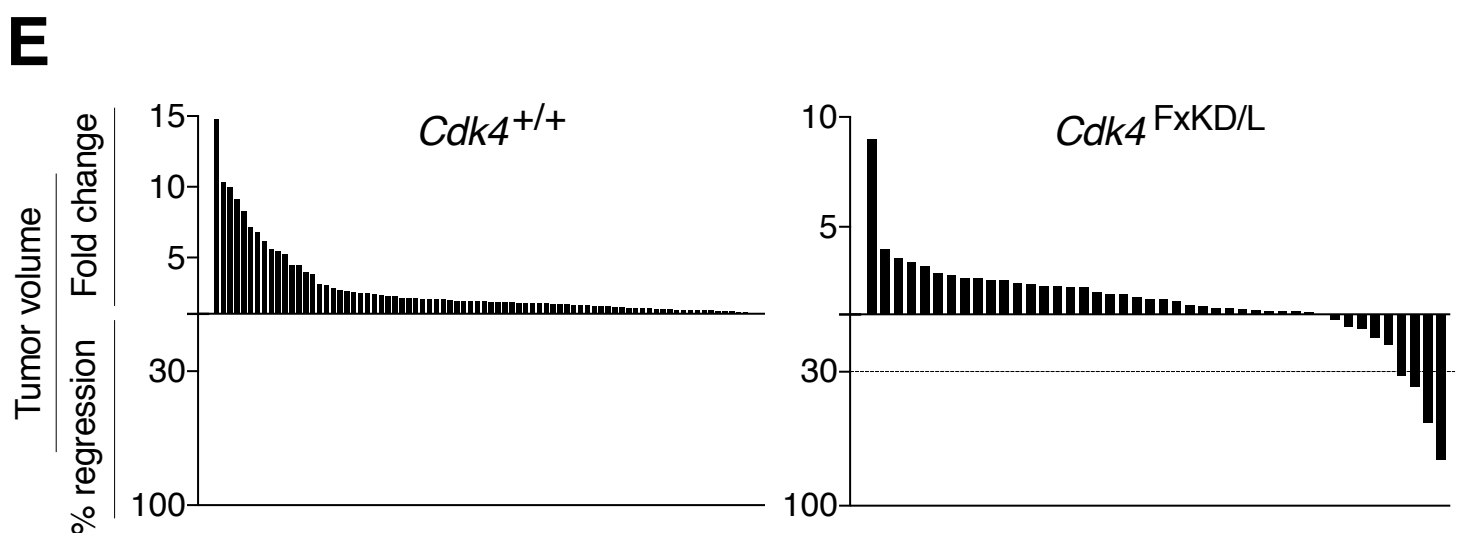
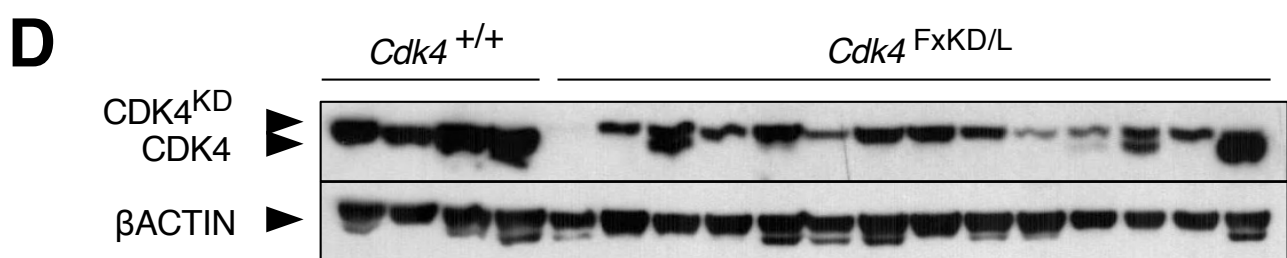
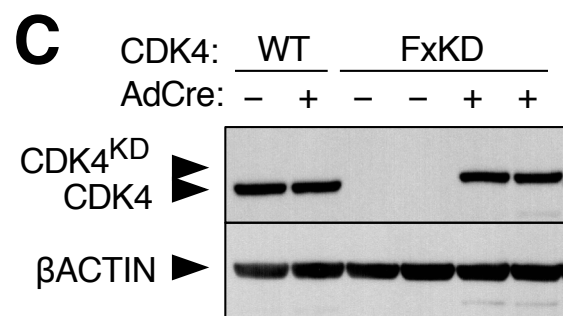
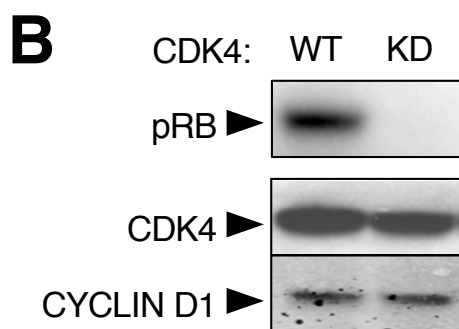
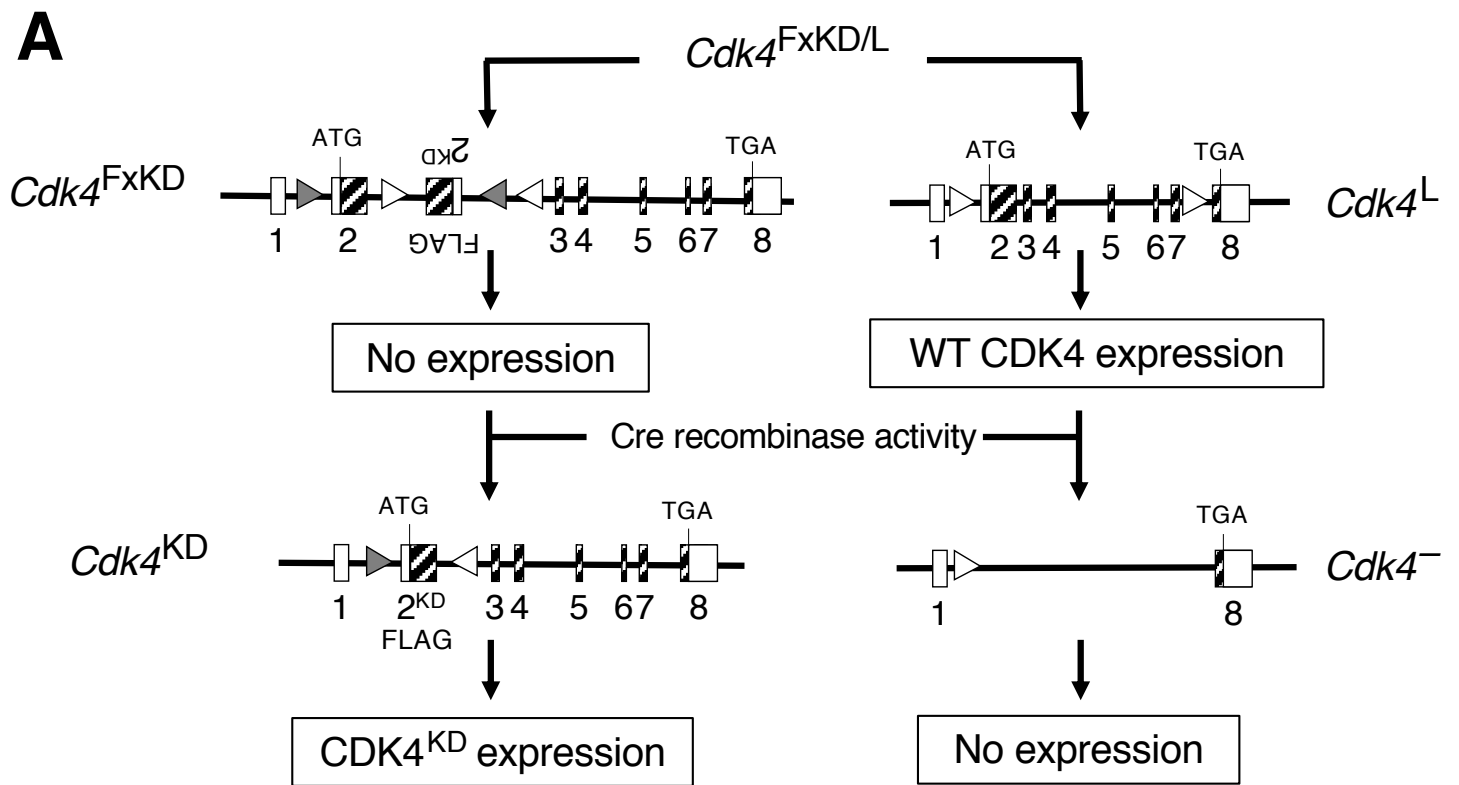


Fig. S1. Expression and anti-tumor effect of a CDK4^{KD} kinase dead isoform. (A) Schematic representation of the conditional *Cdk4^{FxKD}* and *Cdk4^L* alleles and the resulting *Cdk4^{KD}* and *Cdk4⁻* alleles generated upon Cre-mediated recombination. Expression of wild type CDK4 or kinase dead CDK4^{KD} proteins by the corresponding alleles is indicated. (B) Autoradiography of incorporated [³²P]-ATP to recombinant RB protein to determine the kinase activity associated with wild type CDK4 and mutant CDK4^{KD} recombinant proteins incubated with mouse CYCLIN D1 expressed in a baculovirus system as determined by Western blot analysis. Migration of the above proteins is indicated by arrowheads. (C) Western blot analysis of CDK4 and CDK4^{KD} expression in whole cell extracts obtained from *Cdk4^{+/+}* and *Cdk4^{FxKD/FxKD}* mouse embryonic fibroblasts before and after exposure to Adeno Cre (AdCre) particles. βACTIN was used as loading control. Migration of the above proteins is indicated by arrowheads. (D) Western blot analysis of CDK4 and CDK4^{KD} expression in tumor lysates from *Kras^{+FSFG12V};Trp53^{F/F};hUBC-CreERT2^{+/T}* mice harboring *Cdk4^{+/+}* or *Cdk4^{FxKD/L}* alleles after 9 wk of TX exposure. βACTIN was used as loading control. (E) Waterfall plots representing the increase in tumor volume (fold change) and the percentage of tumor regression as determined by CT scans performed at the beginning and at the end of the trial of individual lung tumors present in *Kras^{+FSFG12V};hUBC-CreERT2^{+/T};Cdk4^{+/+}* (n=25mice/85tumors) and *Kras^{+FSFG12V};hUBC-CreERT2^{+/T};Cdk4^{FxKD/L}* (n=19 mice/44 tumors) mice exposed to TX for 9 wk.

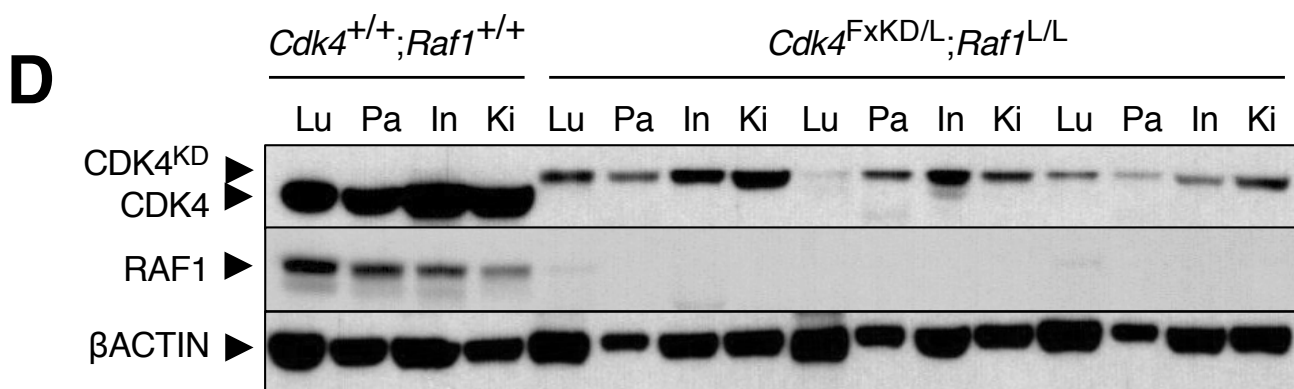
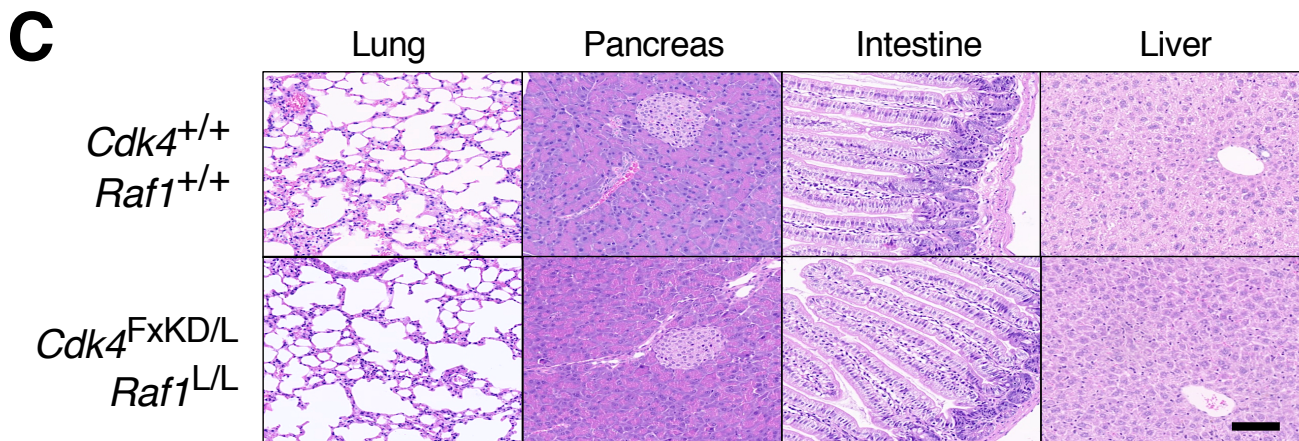
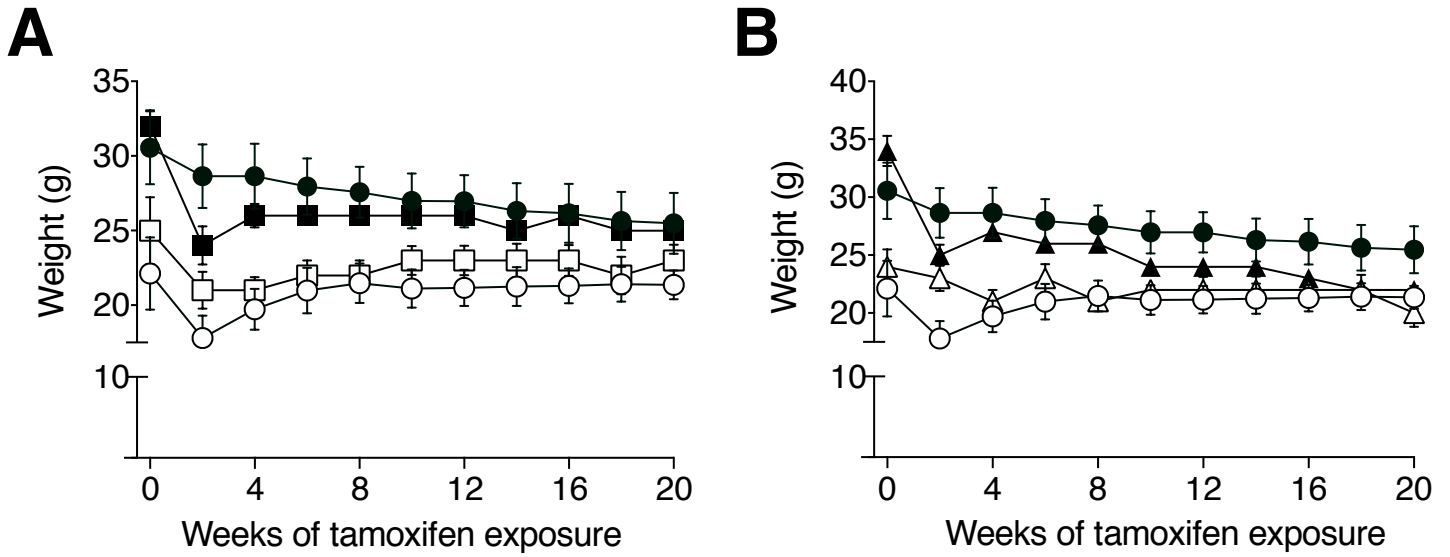


Fig. S2: Limited toxicities upon concomitant CDK4 and RAF1 inactivation in adult mice.

(A) Body weight change in grams (g) of non-tumor-bearing male (solid) and female (open) mice exposed to TX for 20 wk. *hUBC-CreERT2^{+T};Cdk4^{+/+};Raf1^{+/+}* (circles) and *hUBC-CreERT2^{+T};Cdk4^{FxKD/L};Raf1^{+/+}* (squares) mice. n=5 mice/group. Error bars indicate mean \pm SEM.

(B) Body weight change in grams (g) of non-tumor-bearing male (solid) and female (open) mice exposed to TX for 20 wk. *hUBC-CreERT2^{+T};Cdk4^{+/+};Raf1^{L/L}* (circles) and *hUBC-CreERT2^{+T};Cdk4^{FxKD/L};Raf1^{L/L}* (triangles) mice. n=5 mice/group. Error bars indicate mean \pm SEM.

(C) Representative images of H&E stained histological sections of paraffin embedded organs of *hUBC-CreERT2^{+T};Cdk4^{+/+};Raf1^{+/+}* and *hUBC-CreERT2^{+T};Cdk4^{FxKD/L};Raf1^{L/L}* mice sacrificed after 20 wk of continuous exposure to TX. (Scale bar, 0.1 mm.).

(D) Western blot analysis of CDK4, CDK4^{KD} and RAF1 expression levels in tissue lysates obtained from the indicated organs isolated from *hUBC-CreERT2^{+T};Cdk4^{+/+};Raf1^{+/+}* and *hUBC-CreERT2^{+T};Cdk4^{FxKD/L};Raf1^{L/L}* mice after 9 wk of TX exposure. β ACTIN was used as loading control. Migration of the above proteins is indicated by arrowheads. Lu: lung, Pa: pancreas, In: intestine, Ki: kidney.

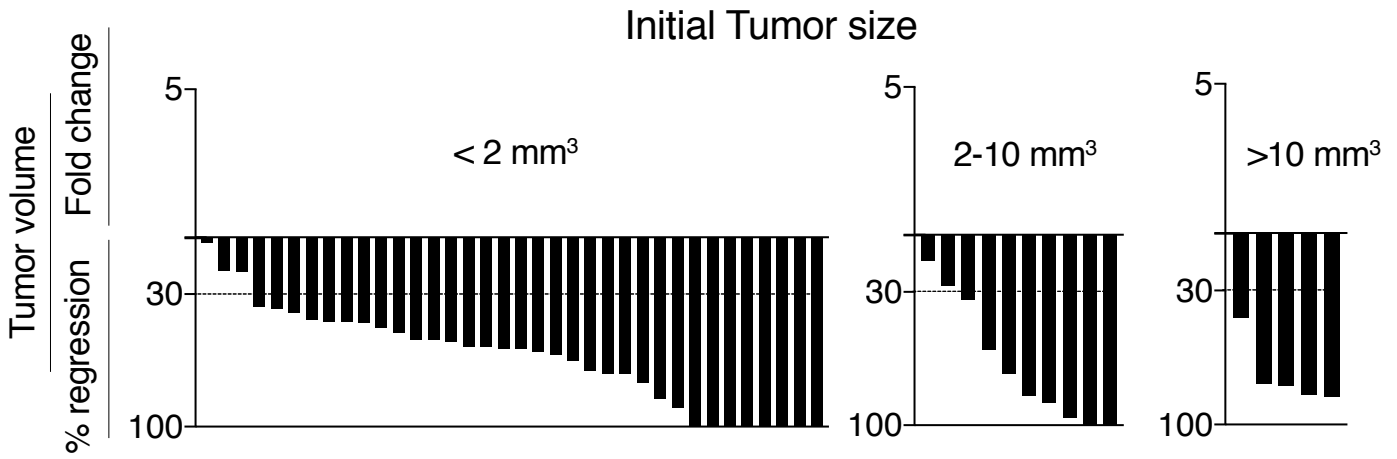
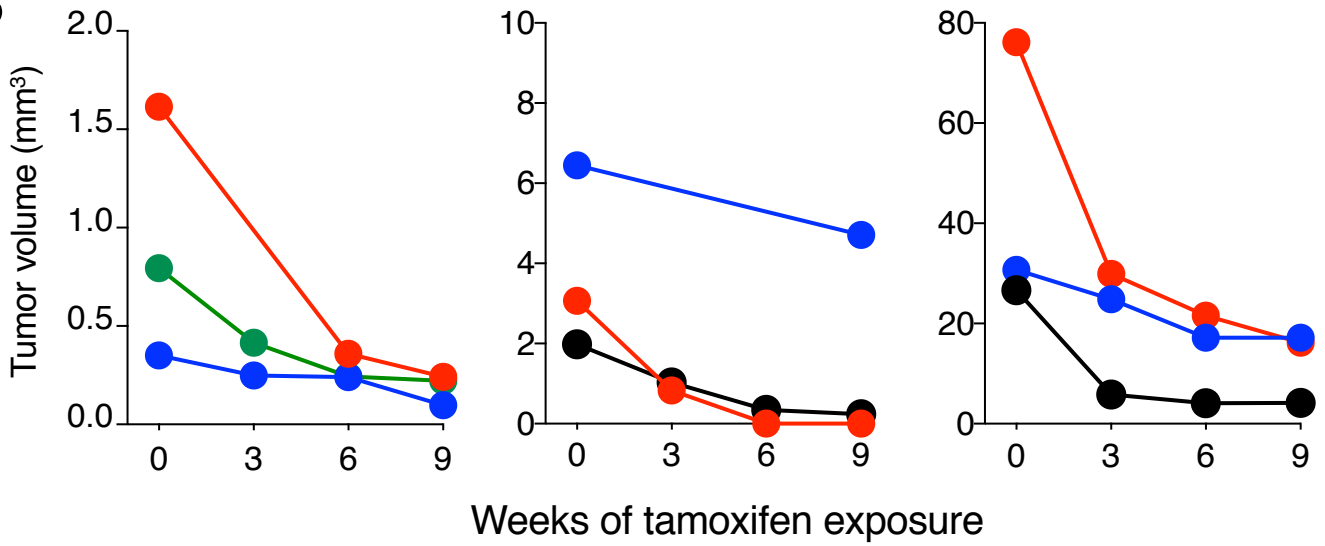
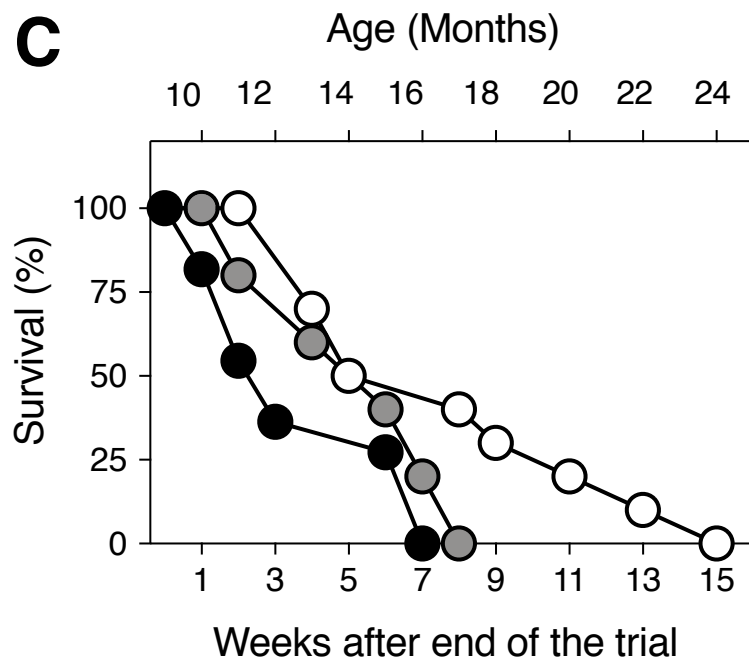
A**B****C**

Fig. S3: Tumor regression upon CDK4/RAF1 inactivation is independent of their initial size. (A) Waterfall plot representing the increase in tumor volume (fold change) and the percentage of tumor regression as determined by CT scans performed at the beginning and at the end of the trial of individual lung tumors present in *Kras*^{+/*FSFG12V*};*Trp53*^{F/F};*hUBC-CreERT2*^{+/*T*};*Cdk4*^{FxKD/L};*Raf1*^{L/L} (n=19 mice/51tumors) exposed to TX for 9 wk and classified according to their initial tumor volume of less than 2 mm³, 2-10 mm³ or more than 10 mm³. (B) Tumor volume monitoring during the 9 wk-long trial of 3 representative tumors from each of the three groups indicated in (A). Each color represents tumors from the same mouse. (C) Survival of *Kras*^{+/*FSFG12V*};*Trp53*^{F/F};*hUBC-CreERT2*^{+/*T*};*Cdk4*^{+/*+*};*Raf1*^{+/*+*} (solid circles; n=11), *Kras*^{+/*FSFG12V*};*Trp53*^{F/F};*hUBC-CreERT2*^{+/*T*};*Raf1*^{L/L} (gray circles; n=6) and *Kras*^{+/*FSFG12V*};*Trp53*^{F/F};*hUBC-CreERT2*^{+/*T*};*Cdk4*^{FxKD/L};*Raf1*^{L/L} (open circles; n=10) mice after the 9 wk-long trial. The upper time scale indicates the age of the mice.

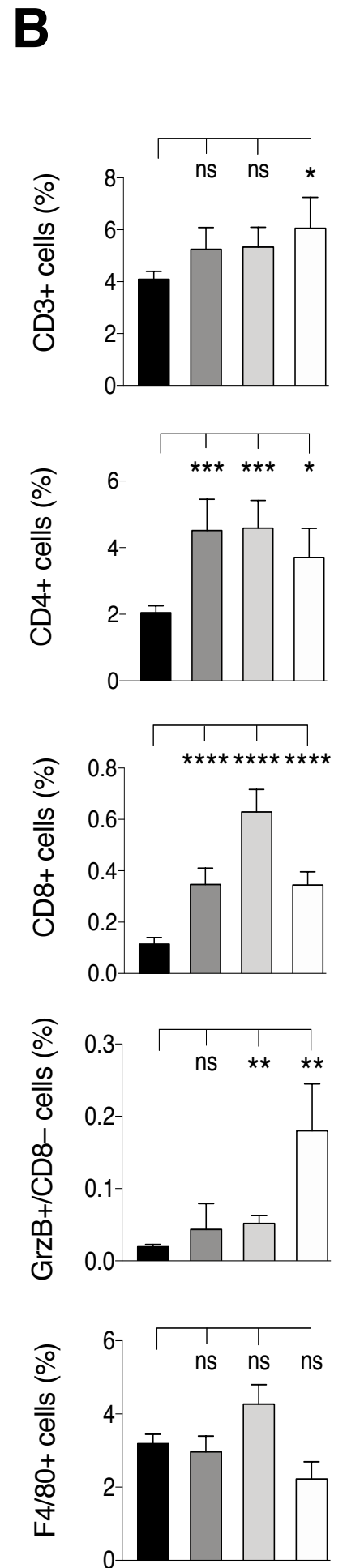
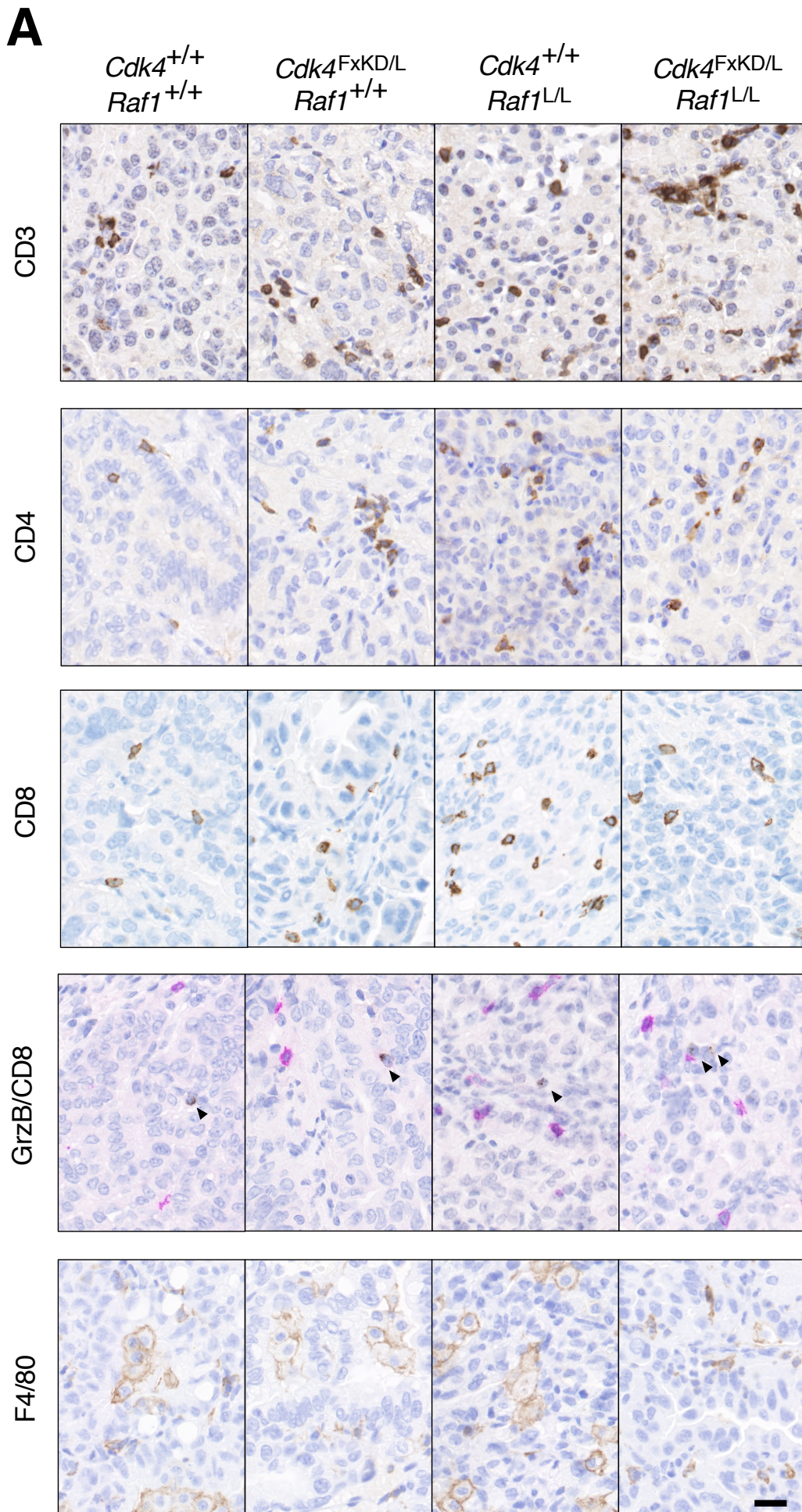


Fig. S4. Immune cell infiltration in tumors upon combined CDK4 and RAF1 inactivation.

(A) Immuno-staining of representative paraffin embedded sections of tumors from *Kras*^{+/^{FSFG12V};Trp53^{F/F};hUBC-CreERT2^{+/^T} mice harboring *Cdk4*^{+/⁺};*Raf1*^{+/⁺}, *Cdk4*^{FxKD/L};*Raf1*^{+/⁺}, *Cdk4*^{+/⁺};*Raf1*^{L/L} and *Cdk4*^{FxKD/L};*Raf1*^{L/L} alleles after 9 wk of TX exposure with antibodies against CD3; CD4; CD8; GranzymeB/CD8 and F480. Scale bar: 0.02 mm. (B) Quantification of the results depicted in (A). Tumors from *Kras*^{+/^{FSFG12V};Trp53^{F/F};hUBC-CreERT2^{+/^T} mice harboring *Cdk4*^{+/⁺};*Raf1*^{+/⁺} (solid bars) (n=3/28tumors), *Cdk4*^{FxKD/L};*Raf1*^{+/⁺} (dark gray bars) (n=3/28tumors), *Cdk4*^{+/⁺};*Raf1*^{L/L} (light gray bars) (n=3/23tumors) and *Cdk4*^{FxKD/L};*Raf1*^{L/L} (open bars) (n=8/28tumors) alleles after 9 wk of TX exposure. *P* values were calculated using the unpaired Student's *t* test. *****P* < 0.0001, ***P* < 0.01, and **P* < 0.05, ns, not significant. (Scale bar, 0.02 mm.)}}

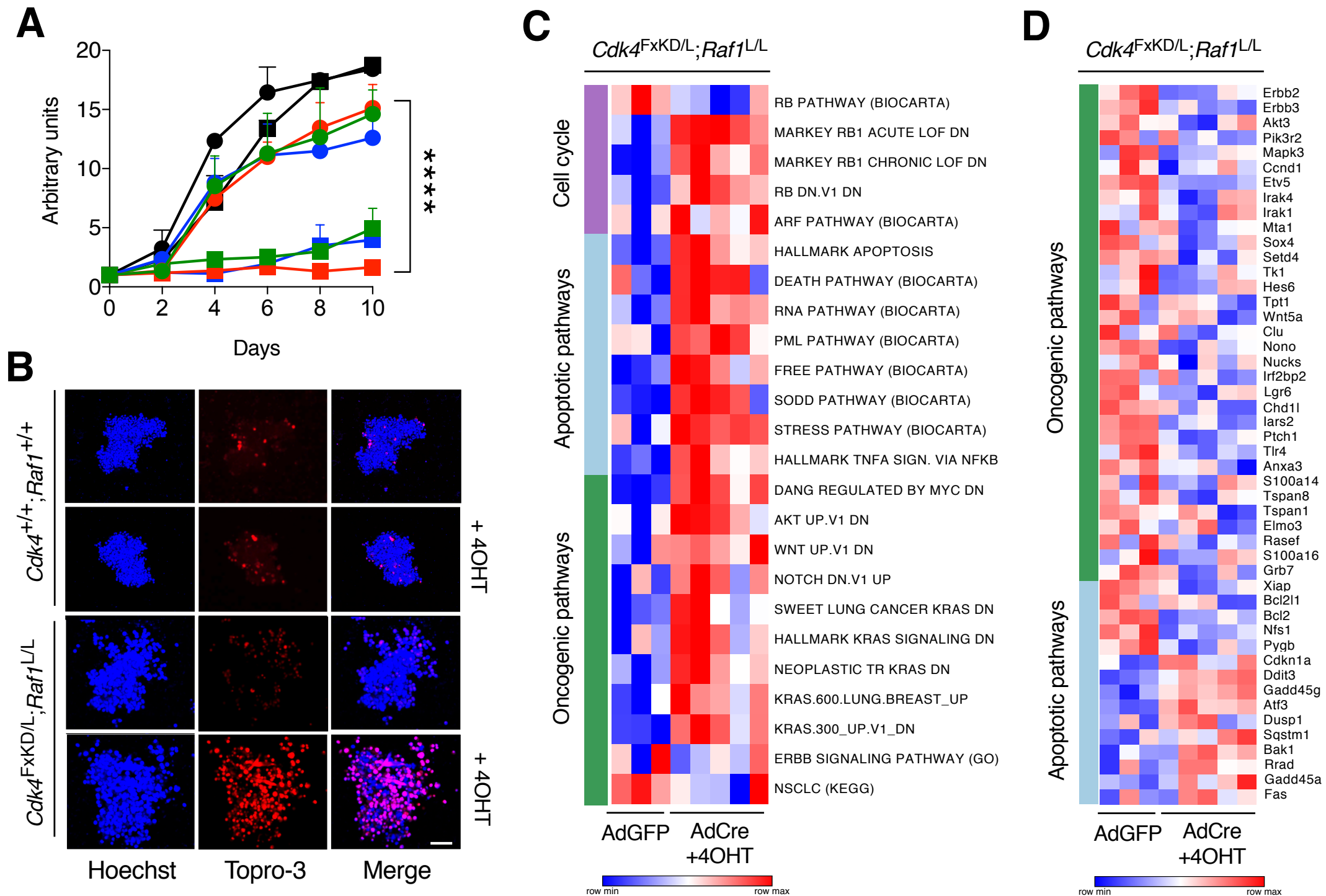


Fig. S5. Concomitant inactivation of CDK4 and RAF1 ablation halts proliferation of lung tumor cells. (A) Proliferation of *Kras*^{+/^{FSFG12V};Trp53^{F/F};hUBC-CreERT2^{+/^T} tumor cell lines harboring *Cdk4*^{+/^{+/+}};*Raf1*^{+/^{+/+}} (black), *Cdk4*^{FxKD/L};*Raf1*^{+/^{+/+}} (blue), *Cdk4*^{+/^{+/+}};*Raf1*^{L/L} (green) and *Cdk4*^{FxKD/L};*Raf1*^{L/L} (red) alleles infected with AdGFP (circles) or with AdCre followed by exposure to 4OHT (squares) to induce recombination of the conditional alleles. Error bars indicate mean \pm SEM. *P* values were calculated using the unpaired Student's *t* test. *****P* < 0.0001. (B) Representative images of TO-PRO-3 and Hoechst stained 3D spheroids derived from *Kras*^{+/^{FSFG12V};Trp53^{F/F};hUBC-CreERT2^{+/^T} lung tumor cells harboring *Cdk4*^{+/^{+/+}};*Raf1*^{+/^{+/+}} or *Cdk4*^{FxKD/L};*Raf1*^{L/L} alleles either untreated or exposed to 4OHT. (Scale bar, 0.1 mm.). (C) Heatmap of ssGSEA normalized enrichment scores (NES) for gene sets related to cell cycle (purple), apoptosis (blue), and oncogenic (green) pathways. Columns represent individual *Kras*^{+/^{FSFG12V};Trp53^{F/F};hUBC-CreERT2^{+/^T};*Cdk4*^{FxKD/L};*Raf1*^{L/L} lung tumor cell lines infected with AdGFP or with AdCre followed by exposure to 4OHT. (D) Heatmap of 48 differentially expressed genes related to apoptosis (blue) and oncogenic (green) pathways. Columns represent the same *Kras*^{+/^{FSFG12V};Trp53^{F/F};hUBC-CreERT2^{+/^T};*Cdk4*^{FxKD/L};*Raf1*^{L/L} cell lines used in (B) infected with AdGFP or with AdCre followed by exposure to 4OHT. Adjusted *P* value < 0.05.}}}}

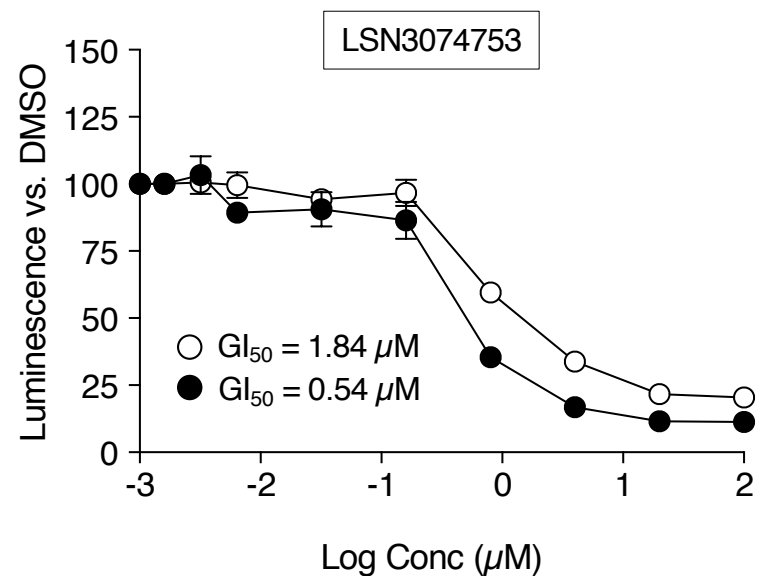
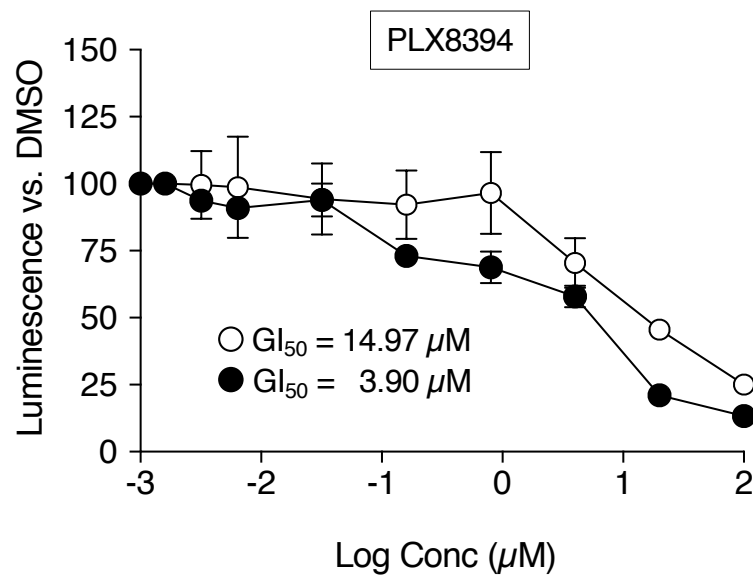
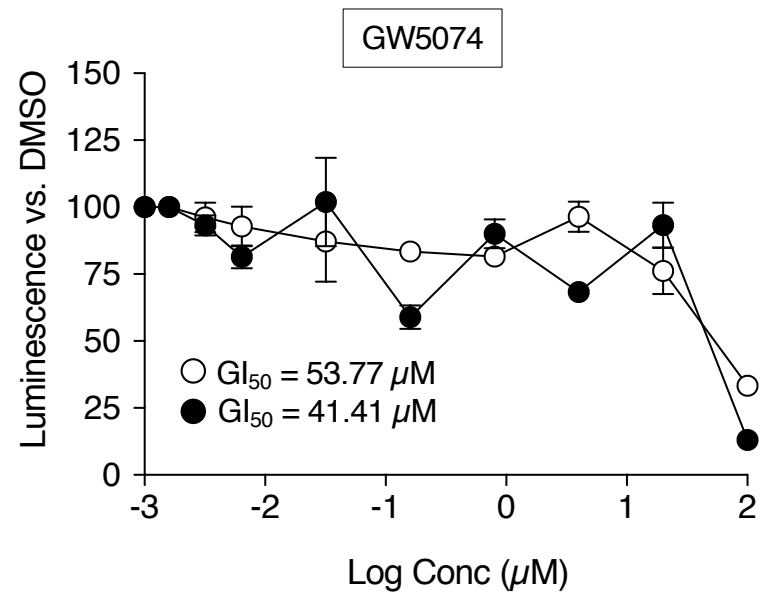
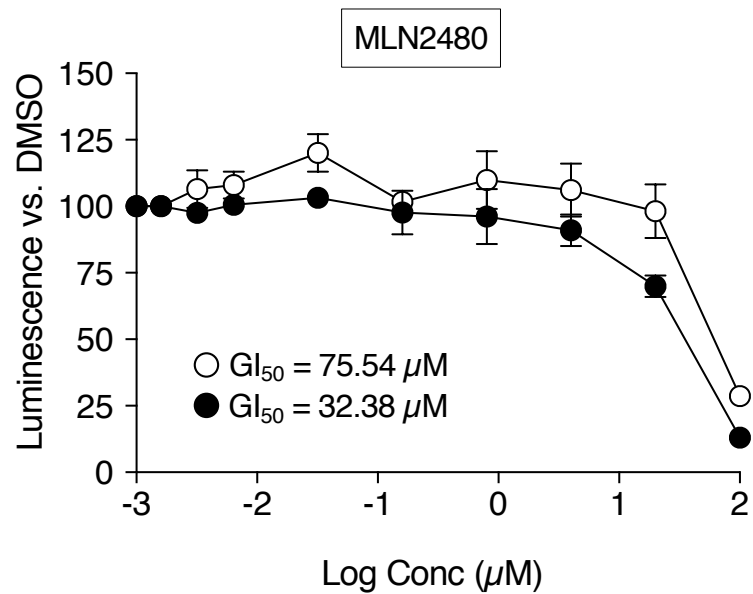


Fig. S6. Effect of panRAF inhibitors in PDX derived lung tumor cell lines. Cell viability assays in PDX-derived cell lines including PDX dc-1 (solid circles) and PDX dc-2 (open circles) treated with 4 different panRAF inhibitors, MLN2480, GW5074, PLX8394 and LSN3074753 for 72h. The GI50 calculated for each cell line is indicated in the figure.

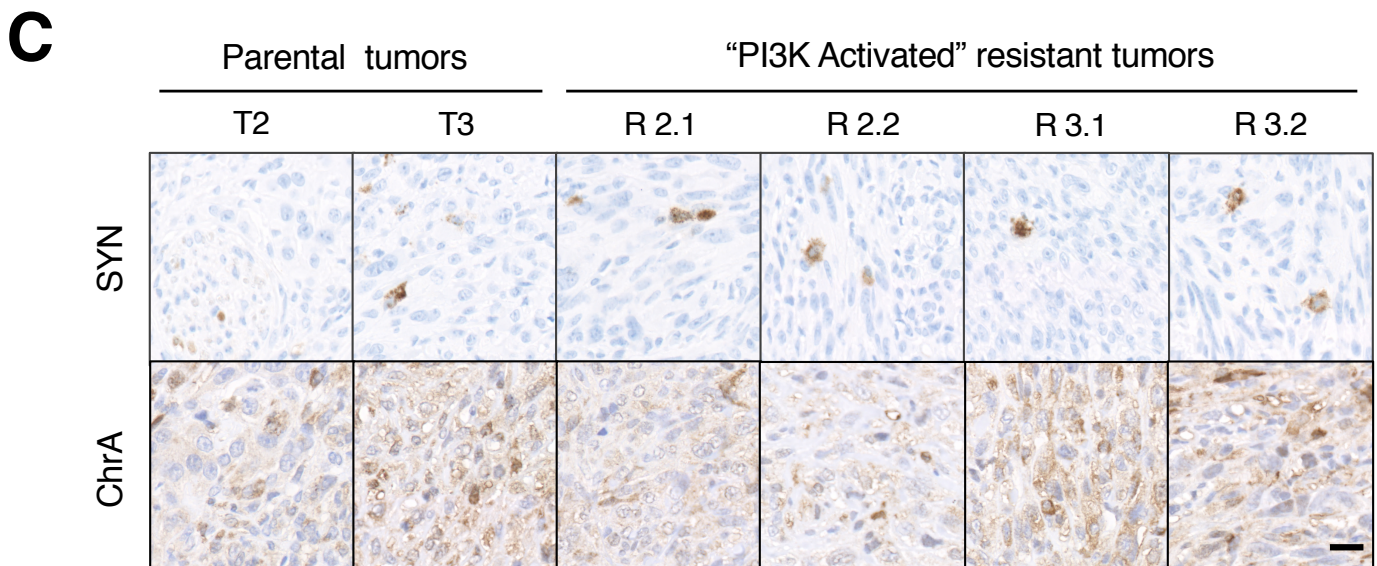
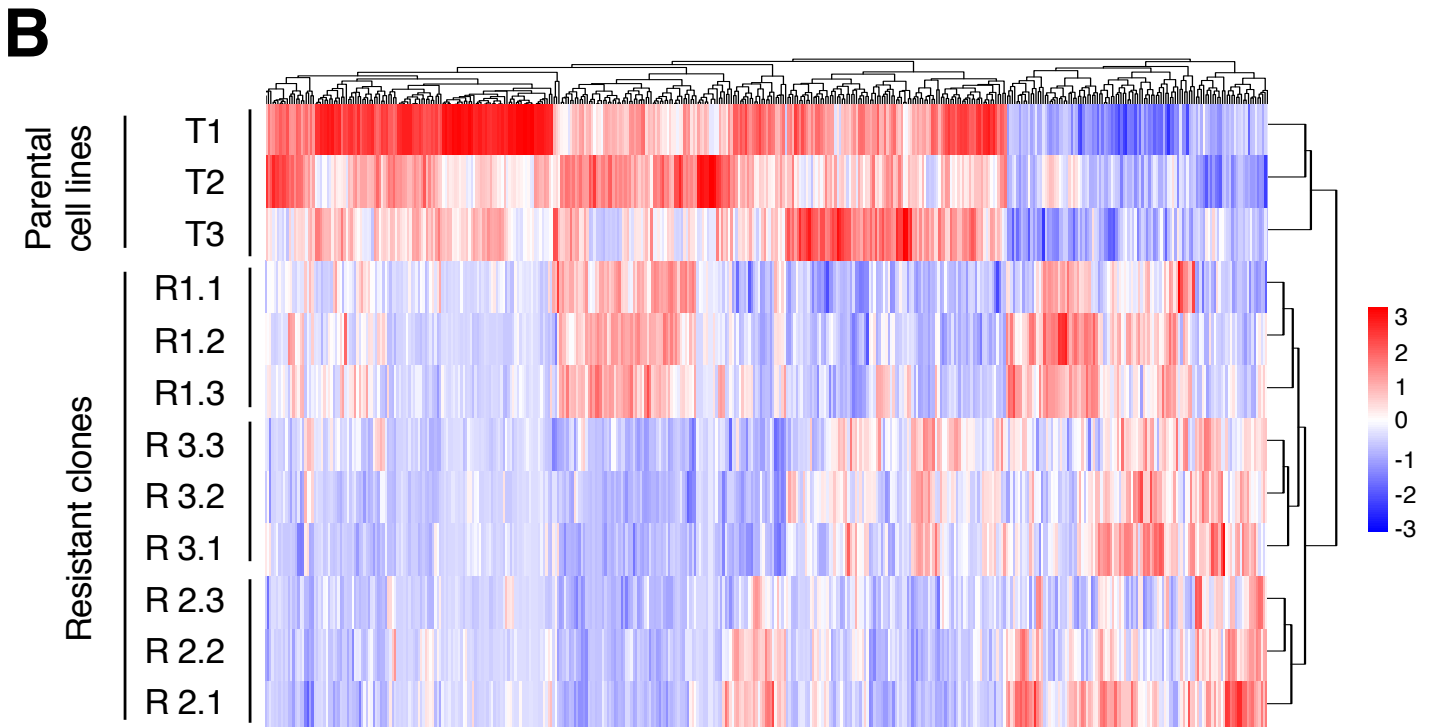
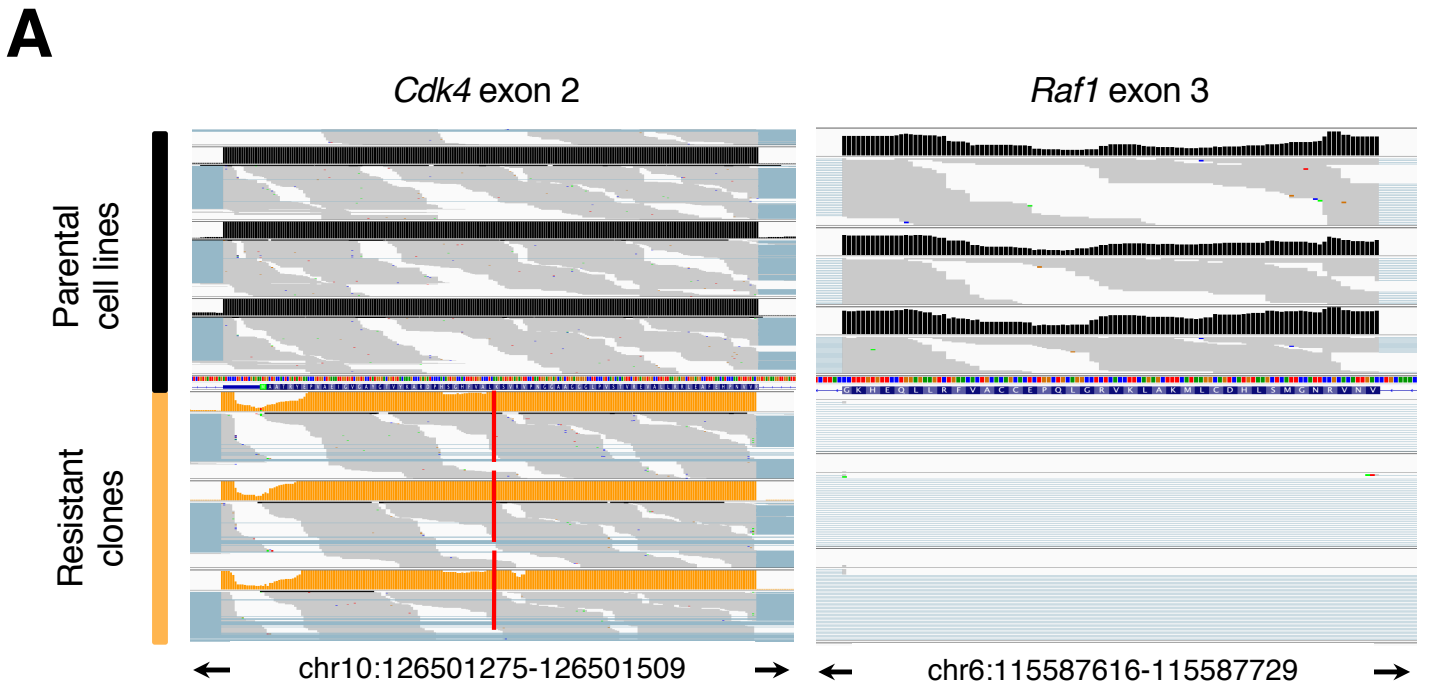


Fig. S7. Transcriptional and phenotypic characterization of CDK4/RAF1 resistant clones.

(A) Short-reads alignments of *Cdk4* exon 2 and *Raf1* exon 3 sequences from RNAseq data mapped to the genome reference (Genome assembly MGSCv37, mm9) in parental cell lines before CDK4 inactivation and RAF1 ablation (solid bars) and in CDK4/RAF1 resistant clones (orange bars). The red lines in *Cdk4* exon 2 show the AAG to ATG mutation responsible for the K35M mutation present in the CDK4^{KD} kinase dead isoform. The lack of sequences in *Raf1* exon 3 reflect the Cre-mediated recombination in the *Raf1*^L alleles responsible for the ablation of RAF1 expression. Three samples for each genotype are shown for illustrative purposes. (B) Heatmap representing color-coded expression levels of differentially expressed genes in CDK4/RAF1 resistant clones (R1.1, R1.2, R1.3, R2.1 R2.2, R2.3, R3.1, R3.2 and R3.3) and their respective parental cell lines (T1, T2 and T3) before CDK4 and RAF1 inactivation. (C) Immuno-staining with antibodies against synaptophysin (SYN) and chromogranin A (ChrA) in paraffin embedded sections of tumors generated from subcutaneously implanted parental (T) cells or CDK4/RAF1 “PI3K Activated” resistant clones (R) in immunodeficient mice. (Scale bar, 0.02 mm.)

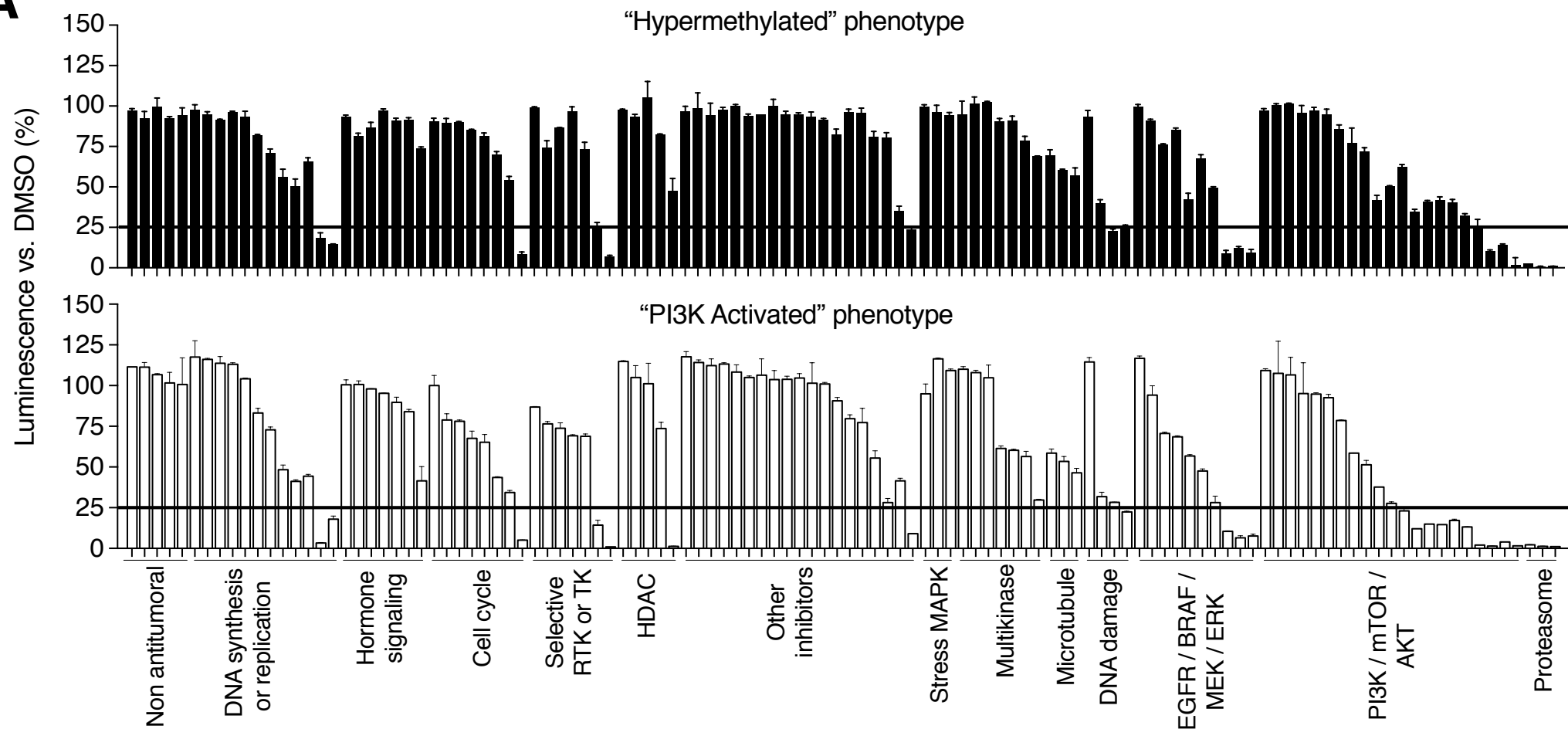
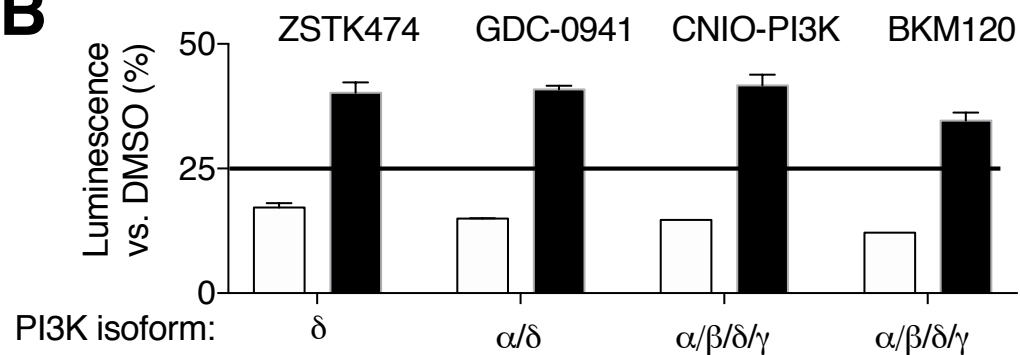
A**B**

Fig. S8. Search for additional drug vulnerabilities in CDK4/RAF1 resistant cells. (A) Cell viability assay of R1 (solid bars) and R2 and R3 (open bars) resistant clones after screening with a library of 114 compounds at a unique 5 μ M dose during 72 hours. The solid horizontal lines represent the cut-off for 25% inhibition (B) Compounds that achieved >75% cell growth inhibition for R2 and R3 resistant clones having a “PI3K Activated” phenotype (open bars) compared to R1 resistant clones having a “hypermethylated” phenotype (solid bars). The designation and PI3K isoform specificity of each compound is indicated. The solid horizontal line represents the 25% inhibition cut-off. Error bars indicate mean \pm SEM.

Table S1. Number of tumors and therapeutic responses observed upon inactivation of CDK4 alone or in combination with RAF1 ablation after 9 weeks of TX exposure. Stable Disease (SD), Partial Response (PR), Complete Response (CR) and Progressive Disease (PD).

Tumor number and therapeutic response	<i>Kras</i> ^{+/FSFG12V} ; <i>hUBC-CreERT2</i> ^{+T} ; <i>Cdk4</i> ^{+/+}		<i>Kras</i> ^{+/FSFG12V} ; <i>hUBC-CreERT2</i> ^{+T} ; <i>Cdk4</i> ^{FxKD/L}		<i>Kras</i> ^{+/FSFG12V} ; <i>Trp53</i> ^{F/F} ; <i>hUBC-CreERT2</i> ^{+T} ; <i>Cdk4</i> ^{+/+}		<i>Kras</i> ^{+/FSFG12V} ; <i>Trp53</i> ^{F/F} ; <i>hUBC-CreERT2</i> ^{+T} ; <i>Cdk4</i> ^{FxKD/L}	
	Number of tumors		Number of tumors		Number of tumors		Number of tumors	
Initial tumor number	105		51		70		31	
Final tumor number	85		44		45		27	
SD (<30%)	0	0%	5	11%	0	0%	1	4%
PR (>30%)	0	0%	4	9%	0	0%	2	7%
CR	0	0%	0	0%	0	0%	0	0%
PD	85	100%	35	80%	45	100%	24	89%

Tumor number and therapeutic response	<i>Kras</i> ^{+/FSFG12V} ; <i>Trp53</i> ^{F/F} ; <i>hUBC-CreERT2</i> ^{+T} ; <i>Cdk4</i> ^{+/+} ; <i>Raf1</i> ^{L/L}		<i>Kras</i> ^{+/FSFG12V} ; <i>Trp53</i> ^{F/F} ; <i>hUBC-CreERT2</i> ^{+T} ; <i>Cdk4</i> ^{FxKD/L} ; <i>Raf1</i> ^{L/L}	
	Number of tumors		Number of tumors	
Initial tumor number	66		56	
Final tumor number	62		51	
SD (<30%)	7	11%	5	10%
PR (>30%)	34	55%	34	66%
CR	6	10%	12	24%
PD	15	24%	0	0%

Table S2. Percentage of allele excision in residual lesions as determined by laser capture microdissection

Tumor	Percentage of allele recombination		
	<i>Cdk4</i> ^L	<i>Cdk4</i> ^{FxKD}	<i>Raf1</i> ^L
T1	77%	94%	100%
T2	99%	98%	85%
T3	100%	94%	100%
T4	98%	98%	95%
T5	100%	85%	100%
T6	100%	80%	98%
T7	100%	100%	100%
T8	100%	35%	99%
T9	79%	56%	100%
T10	83%	36%	84%
T11	100%	55%	98%
T12	95%	27%	98%
T13	99%	55%	99%
T14	100%	60%	99%

Table S3. Compounds used in the drug screening assay described in *SI Appendix*, Fig. S8

	Drug Name		Drug Name		Drug Name			
Non antitumoral	EFLORNITHINE	HDAC	VALPROIC ACID	DNA damage	OLAPARIB			
	SURAMIN		RICOLINOSTAT		KU-57788			
	METFORMIN		PHENYLBUTYRATE		AZ20			
	DISULFIRAM		VORINOSTAT		CNIO-ATR			
	TEMPOL		PANOBINOSTAT		VEMURAFENIB			
DNA synthesis or replication	OXALIPLATIN		Other inhibitors	AICAR	EGFR/BRAF/ MEK/ERK	DABRAFENIB		
	TEMOZOLOMIDE	CNIO-PIM		ERLOTINIB				
	IRINOTECAN	ZILEUTON		GEFITINIB				
	CYCLOPHOSPHAMIDE	FINASTERIDE		LAPATINIB				
	CISPLATINUM	PX-478		GDC-0994				
	LOMUSTINE	EX-527		SELUMETINIB				
	5-FLUORACIL	SILMITASERTIB		PD-0325901				
	MITOMYCIN C	VISMODEGIB,		TRAMETINIB				
	SN-38	GALUNISERTIB		SCH772984				
	ETOPOSIDE VP16-213	SEMAGACESTAT		PERIFOSINE				
	DOXORUBICINE	S-RUXOLITINIB		GSK2636771				
	GEMCITABINE	LY-411575		PF 4708671				
	Hormone signalling	LETROZOLE		SB 505124		PILARALISIB	PI3K/mTOR/AKT	AZD5363
		MIFEPRISTONE		BAY 87-2243		TGX-221		
		GENISTEIN		BARDOXOLONE		IDELALISIB		
ABIRATERONE		ELESCLOMOL	RAPAMYCIN					
KETOCONAZOLE		S7289	BYL-719					
FULVESTRANT		PEMETREXE	MK-2206					
TAMOXIFEN		GELDANAMYCIN	KU-0063794					
Cell cycle		ROSCOVITINE	TANZISERTIB	GEDATOLISIB	BKM120			
	SNS-314 MESYLATE	SB 203580	GDC-0941	PI3K-CNIO				
	TOZASERTIB	DORAMAPIMOD	ZSTK474	BEZ-235				
	ALISERTIB	LINIFANIB	GSK2126458	CNIO-PI3K-2				
	INH CDK4/6	IMATINIB	CNIO-PI3K-3	CUDC-907				
	AT7519	SORAFENIB	IXAZOMIB	Protea- some				
	GSK461364	PAZOPANIB	BORTEZOMIB					
	FLAVOPIRIDOL	CUDC-101	CARFILZOMIB					
Selective RTK or TK	NVP-BGJ398	DOVITINIB	Micro- tubule	DOCETAXEL				
	QUIZARTINIB	DASATINIB		PACLITAXEL				
	LY2801653	DOCETAXEL		VINCRISTINE				
	OSI-906	PACLITAXEL						
	BAY 61-3606	VINCRISTINE						
	TX-1123							
	CRIZOTINIB							